

## Research Article

# An Investigation of Upper Extremity Impedance Modeling and Sensory Thresholds Under Envelope Wave Electrical Stimulation

Renling Zou<sup>1\*</sup>; Yuhao Liu<sup>1</sup>; Yicai Wu<sup>1</sup>; Liang Zhao<sup>1</sup>; Jigao Dai<sup>1</sup>; Xiufang Hu<sup>1</sup>; Xuezhi Yin<sup>2</sup>

<sup>1</sup>University of Shanghai for Science and Technology, Shanghai, 200000, China

<sup>2</sup>Shanghai Berry Electronic Technology Co., Ltd., Shanghai, 200000, China.

**\*Corresponding author: Renling Zou**

University of Shanghai for Science and Technology, Shanghai, 200000, China.

Email: zourenling@163.com

**Received:** March 06, 2024

**Accepted:** April 12, 2024

**Published:** April 19, 2024

## Introduction

As a rehabilitation technique for neurological injury diseases, electrical stimulation therapy has received extensive attention and research in recent years, and it can help patients rebuild or restore some of their motor functions [1,2]. At present, there are more and more forms of electrical stimulation instruments on the market. Most electrical stimulation therapeutic instruments adjust the treatment intensity according to the subjective pain perception of patients [3], and cannot record the physiological information of patients, such as bioimpedance, Surface Electromyography (SEMG) and so on. This physiological information will play an important guiding role in the treatment of patients [4-7].

The electrical model of the human body is very complex [6-20], and the biological passive impedance model contains complex domains [6,18,20,34], which means that both DC and AC should be considered in the selection of waveforms. YinQimin [9] there is a problem in comparing square waves with differential waves in experiments, because square waves stimulate the

## Abstract

The main purpose of this paper is to study the effect of impedance values and electrical stimulation sensory thresholds of human upper limb sites on the parameter settings of electrical stimulation equipment in low and medium frequency envelope electrical stimulation therapy. By adjusting the modulation wave frequency, carrier frequency and current intensity of the output, different parts of the upper limbs of 22 healthy subjects (age: 21~25 years old, 11 males and 11 females) were tested. Five kinds of electrodes of different sizes were used in the test. In the human upper limb impedance test, the range of impedance values measured by different sized electrodes varies widely. A new impedance model of the human upper limb proposed can fit the relationship between frequency and impedance values very well. In electrical stimulus sensory experiments, the Voltage Perception Threshold (VPT) measurement proposed in this study can be used as a new measure of electrical stimulus sensation. Compared with the Current Perception Threshold (CPT), the effects of current magnitude and output frequency will no longer be considered. The range of sensory thresholds was 6 ~ 8 V; the range of suprathreshold was 9 ~ 11 V. Neither experiment showed gender differences. Determining the value of the power supply and the output intensity of the device power amplification circuitry based on the VPT can provide a precise therapeutic dose for electrical stimulation therapy.

**Keywords:** Electrical stimulation; Human impedance; Voltage perception threshold; Envelope

human body to form differential waves [8,10]. It is impossible to judge the effect of the two waveforms by comparing two different differential waves. One of the ideas we put forward here is that the sensation to the stimulus does not mean that the waveform is not distorted. Many works lack the measurement of relevant physiological information before setting electrical stimulation parameters. YinQimin [9] simply mentions that the impedance range of the human body is 1- 3K $\Omega$ , but the source of this impedance range is not specified. YuZhou [11] did not mention the measurement of the impedance of the human body before designing the boost voltage source. Boosting the power supply to a certain value without determining the impedance value of the human body will cause excessive circuit power consumption or output waveform distortion of the electrical stimulation equipment.

Pain and tolerance threshold can also be regarded as a kind of physiological information, which has important clinical value in evaluating neurological defects, choosing treatment and

recording sensory recovery after injury [21]. Electrical stimulation is a simple method for measuring pain sensation [21-26]. Previous studies have mostly used Current Perception Threshold (CPT) as a criterion [27-34]. The results of Shivayogi [30] show that the receptive intensity increases with the increase of pulse amplitude and frequency, but there is little research on the reasons for the differences in CPT among people of different genders and ages, because the adjustment of electrical stimulation intensity is usually based on subjective verbal commands, and the stimulation waveform, electrode size and other information are sometimes not provided or the parameters are not uniform. It is unreliable to give stimulus dose based on patients' subjective feelings, and how to objectively quantify pain is worth studying. Shin-ichiro [22] measured CPT with five sizes of electrodes. The results showed that the measured values of each electrode increased with the increase of electrode size. By adjusting body fat rate or body water rate, the logarithmic conversion value no longer showed any gender difference of electrode pairs.

The size of the impedance value of the human upper limb will directly affect the size of the supply voltage of the stimulation equipment, and the electrical stimulation sensory threshold affects the setting of the stimulation parameters and the therapeutic effect. In order to investigate the influence of human upper limb impedance value and electrical stimulation sensory threshold on the parameter setting of electrical stimulation equipment, the present study was conducted by controlling variables method to obtain this two physiological information. The variables contain: five different sizes of hydrogel electrodes; modulating waveforms of 2 ~ 150 Hz; carrier waveforms of 1 ~ 10 kHz output waveforms; and output currents of 0 ~ 20 mA. The rest of the paper is as follows: chapter 2 describes the background of the study, analyzes the reasons for considering physiological information in the electrical stimulation parameters, and gives a brief description of the experimental equipment. Chapter 3 includes experiments on human impedance measurement and electrical stimulation perception measurement, and proposes a new human upper limb impedance model and a new electrical stimulation perception measurement method on the experimental results. It concludes with a discussion section.

Materials and Methods

Background

Figure 1 shows a model of a constant current source circuit used in electrical stimulation equipment. The magnitude of the current to stimulate the body can be calculated by equation (1)

$$I_d = I_2 = \frac{U_{in}}{R_{set}} \tag{1}$$

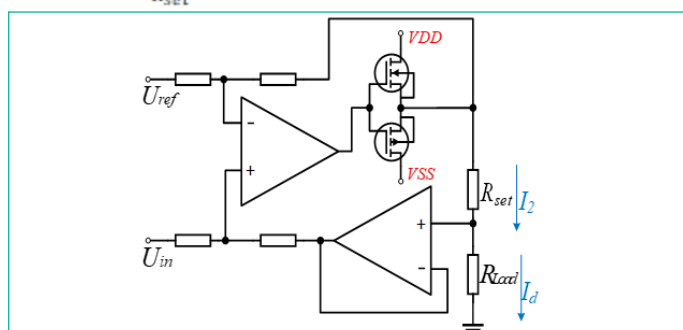


Figure 1: Constant current source model of the electrical stimulation device. RLoad is the impedance of the human upper limb, I\_d is the current flowing through the body, Uin is the input voltage signal.

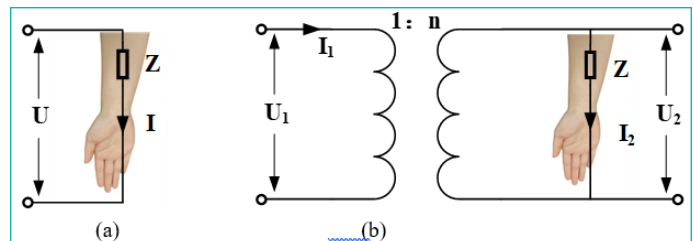


Figure 2: The relationship between the impedance of human body and the power supply of power amplifier circuit. (a):  $U=Z*I$ ; (b):  $U1=U2/n=Z*I2/n$ .

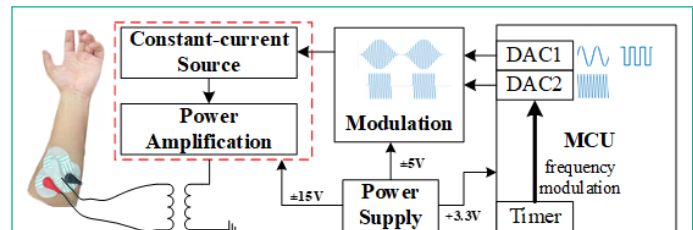


Figure 3: Functional block diagram of electrical stimulation module. It includes MCU, modulation waveform, constant current source output and power amplifier module. The modulation waveform module has two kinds of modulation waveforms.

Here  $I_d$  for the current flowing through the human body ( $R_{load}$  for the impedance of the human upper limb impedance),  $U_{in}$  for the input voltage signal, VDD for the power supply of the power amplifier circuit in the device.  $U_{ref}$  to ground, the output current size is determined only by the input voltage  $U_{in}$  size, and the size of the load  $R_{load}$  has nothing to do.

The relationship between the power supply of the power amplifier module and the impedance amplitude of the human body can be simplified to the model shown in Figure 2a. Previous studies have shown that the intensity of electrical stimulation is usually determined by the current magnitude. When the output current  $I$  is determined, the value of the power supply  $U$  is determined by the maximum value of the impedance  $Z$ . If  $U < Z * I$ , the output waveform will be damaged. If  $U < Z * I$ , it will lead to distortion of the output waveform; if  $U$  is too large, it will increase the power consumption of the whole circuit. Therefore, before determining the value of the power supply, it is necessary to determine the range of the human impedance value. In order to prevent the output waveform from being distorted or the  $U$  value from being set too large during the measurement process, the human impedance value was first measured in this study using the circuit shown in Figure 2b. A transformer is added between the constant-current source power amplifier circuit and the human body load. The transformer isolates the connection between the human body and the circuit board and acts as an impedance transformer. By transforming the large impedance on the load side to a small impedance on the output side, a smaller supply voltage can be

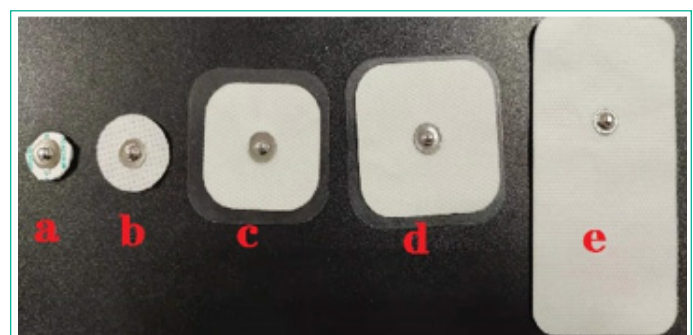


Figure 4: Five kinds of hydrogel electrodes of different sizes. The size parameters of each electrode sheet are: a, 3.53cm<sup>2</sup>; b, 9.82cm<sup>2</sup>; c, 16 cm<sup>2</sup>; d, 25 cm<sup>2</sup>; e, 50 cm<sup>2</sup>.

used without increasing the power consumption of the circuit. In this study the power supply  $U_1=15V$  and the number of turns on the secondary pole of the transformer is selected to be 20, then the maximum undistorted voltage that can be measured on the load side of the human body is 300 V. The power supply voltage can be adjusted at a later stage according to the measured impedance value.

### Principle of Instrument

This device uses the electrical stimulation output as a constant-current source output, and the constant-current source output ensures that the output current will not be affected by changes in the impedance of the human upper limb. Figure 3 shows the functional block diagram of the electrical stimulation module, including MCU, modulation module, constant current source output and power amplification modules. The DAC1 output of the MCU serves as the waveform of the modulating waveform, which can be selected as a sinusoidal waveform or a square waveform. Due to the complex impedance characteristics of the human body, the square wave output will become a differential wave, so DAC2 only outputs AC signals. The frequency of the waveform can be modulated by adjusting the timer. MCU two DAC outputs to add a voltage follower to improve the bandwidth capacity, it is necessary to convert the DAC1 output to  $0 \sim 1 V$ , DAC2 output to  $-1 \sim 1 V$ , and then through the AD835 multiplier will be the two waveforms modulation output to obtain the two kinds of waveforms as shown in the modulation module. Finally, the human body is electrically stimulated through the electrode pads via a constant current source and power amplification.

Before the experiment, it is necessary to evaluate the output capability of the constant current source, using a 100 Hz sinusoidal modulating waveform, a 2 kHz sinusoidal carrier waveform, outputting a constant current, and determining the voltage at its two ends through resistive loads of different resistance values. The output current strength was set to  $5 \sim 25$ , divided into 5 steps. The nominal resistance value of the load is  $1 \sim 5 K\Omega$  (power 50W, accuracy 1%), and the above loads are measured one by one. Table 1 for the measurement results and its average value and standard deviation, the maximum standard deviation of 0.17 mA, basically meet the requirements of constant current source

**Table 1:** Output current values corresponding to different resistance loads and their average values and standard deviations.

		Current intensity /mA				
		5	10	15	20	25
Load/ $\Omega$	1K	5.10	10.8	15.20	20.40	25.40
	2K	5.15	10.2	15.00	20.20	25.20
	3K	5.00	9.98	14.96	19.96	24.88
	4K	4.10	10.10	15.10	20.10	25.12
	5K	5.08	10.20	15.20	20.28	25.26
Statistics	mv	5.08	10.18	15.09	20.19	25.17
	sd	0.05	0.14	0.10	0.15	0.17

**Table 2:** Peak frequencies corresponding to impedance minima, maxima, and maxima measured by the two test groups in the carrier frequency range of 100 ~ 10000 Hz (standard deviation in parentheses).

Area/ $cm^2$	Male(n=11)					Female(n=11)				
	3.53	9.82	16	25	50	3.53	9.82	16	25	50
Min/ $K\Omega$	0.51 (0.05)	0.45 (0.04)	0.39 (0.04)	0.34 (0.05)	0.27 (0.02)	0.51 (0.04)	0.44 (0.03)	0.42 (0.03)	0.38 (0.04)	0.31 (0.02)
Max/ $K\Omega$	21.80 (3.52)	10.98 (3.53)	8.06 (0.89)	6.18 (0.56)	3.79 (0.32)	19.80 (3.18)	11.68 (2.82)	8.16 (0.79)	5.56 (0.57)	3.29 (0.29)
Peak fre/Hz	2000	1500	700	500	400	2000	1500	700	500	400

### Experiments and Results

The experiment used five different sizes of hydrogel electrode pads shown in Figure 4 to conduct the following two tests: 1) output a fixed current size, adjust the modulating wave frequency and carrier frequency, and obtain the impedance value of the upper limb site according to Ohm's law by measuring the voltage in different parts of the upper limb. 2) output currents of different sizes and frequencies to quantify the pain perception threshold. The subjects were 11 healthy male subjects (age  $23 \pm 2$  years, height  $173.2 \pm 5.1$  cm, weight  $70.8 \pm 13.2$  Kg) and 11 healthy female subjects (age  $22 \pm 2$  years, height  $163 \pm 4.7$  cm, weight  $52 \pm 8.6$  Kg). All subjects volunteered and were informed of the purpose of the experiment, and all participants were informed that they could stop the experiment at any time.

#### Human Upper Limb Impedance Measurement

For the measurement of human upper limb impedance, the following aspects were taken into account: different parts of the human upper limb, modulating wave frequency, carrier frequency and electrode size. As shown in Figure 5, the positive electrode of the differential electrode pair was fixed on the left brachioradialis site, and the negative electrode was placed on the following four different sites: (a) for the left brachioradialis muscle, (b) for the left biceps brachii muscle, (c) for the right brachioradialis muscle, and (d) for the right biceps brachii muscle. The electrodes were Ag/AgCl disposable cardiac electrode sheets, the modulating waveform was a 10 Hz sine wave, and the carrier waveform was a 1000 Hz sine wave. During the experiment, the modulating wave frequency was adjusted in steps of 1 Hz within the range of  $2 \sim 150$  Hz, and the results were all about 19.2 V. Therefore, different positions of the upper limb and changing the modulating wave frequency had almost no effect on the value of human impedance. have no effect, therefore, only the relationship between the variables of carrier frequency and electrode size and the impedance of the upper limb were considered in this experiment.

**Measurement result:** The carrier frequency was adjusted in steps of 100 Hz for adjustments within 100 ~ 1000 Hz, 500 Hz for adjustments within 1 ~ 3 kHz, and 1000 Hz for adjustments within 3 ~ 10 kHz. Measurements were made sequentially with five electrode pads. Tests were performed on 11 males versus 11 female subjects, respectively. As shown in Figure 6, Figure 6a shows the test results of the male group and Figure 6b shows the test results of the female group. The results show that the impedance values measured using electrodes of different sizes differ greatly, but the change rule is similar. With the increase of carrier frequency, the impedance value first reaches the peak value, and then decreases with the increase of carrier frequency. And the larger the electrode size, the smaller the carrier frequency corresponding to the peak impedance. When the carrier frequency is greater than 5 kHz, the impedance value tends to flatten out. No differences were shown between genders. Table 2 lists the three impedance eigenvalues for the two test groups,

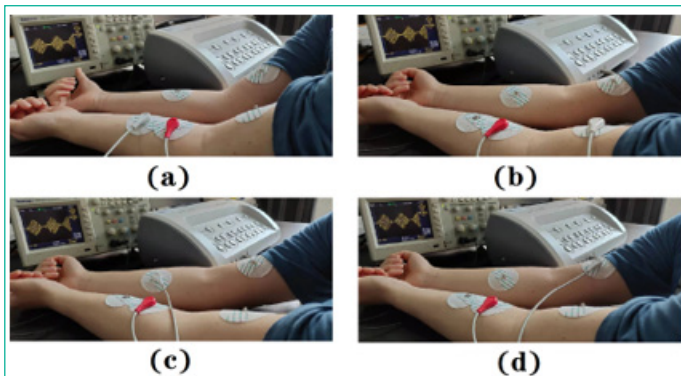


**Figure 5:** Impedance measurements were performed on different positions of the upper limb, the four positions are: **a):** left brachioradialis-left brachioradialis; **b):** left brachioradialis-left biceps brachii; **c):** left brachioradialis-right brachioradialis; **d):** left brachioradialis-right brachioradialis.

**Table 3:** Human body impedance measurement data obtained from five electrodes. The maximum impedance value measured by each electrode of  $Z_{max}$ ,  $f_{peak}$  is the peak frequency corresponding to  $Z_{max}$ .

Electrode/cm <sup>2</sup>	$Z_{min}/K\Omega$	$Z_{max}/K\Omega$	$f_{peak}/Hz$
EL 1	0.51	20	2000
EL 2	0.45	11	1500
EL 3	0.4	8	700
EL 4	0.39	6	500
EL 5	0.29	3.5	400

**Table 4:** Fitted values for each passive device in the circuit model.

Area/ cm <sup>2</sup>	L/H	C/nF	$R_2/\Omega$	$f_{peak}/Hz$	$Z_{max}/K\Omega$
EL 1(3.53)	0.6817	10.41	3178	1890	20.60
EL 2(9.82)	0.6839	22.27	2238	1290	13.72
EL 3(16)	0.7719	75.75	1204	659	8.46
EL 4(25)	0.7306	121.50	934.4	534	6.43
EL 5(50)	0.6777	261.30	659.7	378	3.93

**Table 5:** Pain perception value of a subject by adjusting current at different electrode sizes and different carrier frequencies.

Area/cm <sup>2</sup>	Perception	carrier frequency/KHz					MV	SD	
		6	7	8	9	10			
EL1	Readout (Vpp)	subthreshold	8.4	8	9.4	8.4	8	8.44	0.51
		threshold	11	10.4	11	11.2	10.2	10.76	0.39
		superthreshold	20	20.8	21.6	22	20	20.88	0.82
EL2	Readout (Vpp)	subthreshold	9.2	9.8	9.2	10	9.2	9.48	0.35
		threshold	11	10	10.6	10	10.5	10.42	0.38
		superthreshold	15.8	15.6	14.4	13.4	16	15.04	0.99
EL3	Readout (Vpp)	subthreshold	6.8	6.8	7.68	7.6	6.72	7.12	0.42
		threshold	7.44	7.6	8	8.12	7.12	7.66	0.37
		superthreshold	9.68	9.68	10.2	9.68	9.84	9.82	0.20
EL4	Readout (Vpp)	subthreshold	7.12	6.4	7.2	8.12	6.72	7.11	0.58
		threshold	7.92	7.12	7.92	8.6	7.44	7.80	0.50
		superthreshold	9.68	9.6	10.6	10.7	9.6	10.04	0.50
EL5	Readout (Vpp)	subthreshold	6.16	5.84	6.4	6.72	7.44	6.51	0.55
		threshold	7.2	6.4	7.12	7.44	7.92	7.22	0.49
		superthreshold	9.68	10.2	9.52	10.1	9.52	9.8	0.29

which are the impedance minima, maxima, and peak frequencies corresponding to the impedance maxima measured for each electrode size. The peak frequencies were identical and the impedance values did not differ significantly by gender.

**Human Upper Limb Impedance Model:** According to the analysis of the experimental data, there is a maximum impedance peak at a certain frequency, and the three-element equivalent circuit model proposed by Cole is widely used in the current analysis of human impedance, as shown in the circuit model

in Table 6. In the circuit model of RC, it is not possible to have impedance peaks, therefore, in the case of electric stimulation of the envelope waveform formed by the modulating waveform and the carrier waveform, the traditional human impedance model is not applicable, and for the low and medium frequency envelope waveform electric stimulation, a suitable passive circuit model is used to fit the data, and the values of the parameters related to the impedance of the upper limb of the human body can be further analyzed. According to the human upper limb impedance change rule shown in Figure 6, it indicates that in the upper limb not only has capacitive characteristics, there may also exist the characteristics of inductance, inductance and capacitance under the joint action of the resonance frequency there is a peak value of the impedance. In this study, the human upper limb impedance model shown in Figure 7 is proposed.

**Table 6:** Five impedance models of human body.

Definition	Model	References
Montague		[18]
Tregear		[18]
CPE_based		[18]
Three-element		[6.20]
FOIM		[34]

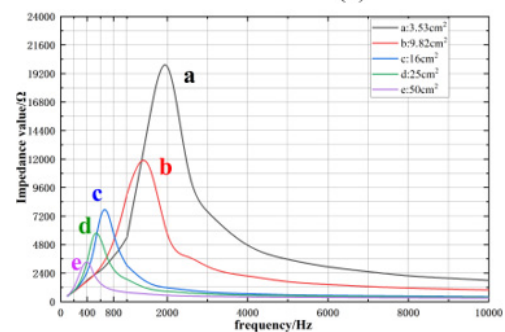
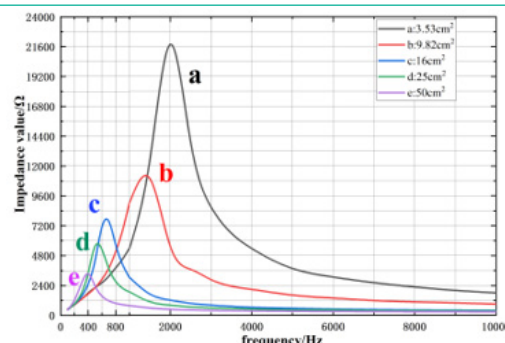


**Figure 6:** Impedance value versus carrier frequency (100 ~ 10000 Hz), five electrode sizes. step frequency is 100 Hz in 100 ~ 1000 Hz; step frequency is 500 Hz in 1 ~ 3 KHz; and step frequency is 1000 Hz in 3 ~ 10 KHz. **(a)** is the result of male measurement and **(b)** is the result of female measurement.

The expression for the impedance value Z is:

$$Z = R_1 + \frac{1}{j\omega C} // (R_2 + j\omega L)$$

$$= R_1 + \frac{\frac{1}{j\omega C}(R_2 + j\omega L)}{j\omega L + R_2 + \frac{1}{j\omega C}} \quad (2)$$

In order for the model to reach the peak frequency, let  $R_2 \ll \omega L$ , then the expression of Z is:

$$Z \approx R_1 + \frac{\frac{L}{C}}{R_2 + j(\omega L - \frac{1}{\omega C})} \quad (3)$$

When  $\omega L = \frac{1}{\omega C}$ , The impedance value Z is the highest, and the maximum value  $Z_m \approx \frac{L}{R_2 C}$ . The peak frequency at this time  $f_{peak} = \frac{1}{2\pi\sqrt{LC}}$ . Table 3 lists the relevant data measured in the experiment.

Figure 7 shows the fitting result of formula (3) to the imped-

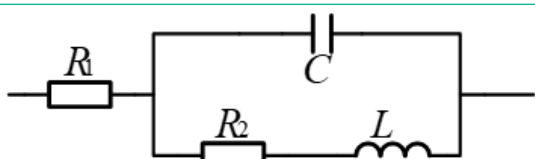


Figure 7: Passive circuit model of human impedance.

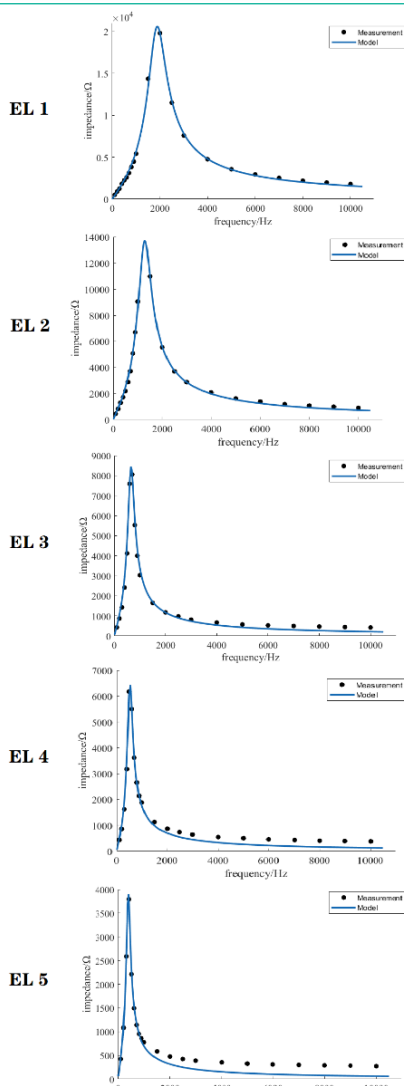


Figure 8: Fitting result of equation (3) for impedance value and its corresponding frequency. The solid point is the measured data and the solid line is the fitting curve.

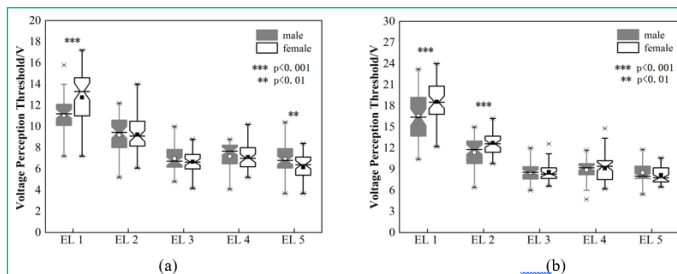


Figure 9: Compares the Voltage Perception Threshold (VPT) obtained by male (gray) and female (white) subjects using five sizes of electrodes. (a) and (b) represent sensory threshold and supra-sensory threshold, respectively. The frame limits are the 25<sup>th</sup> and 75<sup>th</sup> percentiles. The beard indicates an outlier. A small box represents an average. The notch is the median, and \* indicates that there are significant differences between sexes (\*\*\*) p<0.001, \*\*p<0.01).

ance value and its corresponding frequency. Twenty-one discrete points are obtained from each electrode, and the solid line represents the fitted curve. Table 4 shows the fitted values of the components in the circuit model and the theoretical peak frequencies and impedance maxima calculated from the fitted values. The results are analyzed that the inductance L is almost a fixed value, the fitted value of capacitance C increases with increasing electrode size and the fitted value of resistance  $R_2$  decreases with increasing electrode size. A linear relationship is satisfied between Area, C, and  $R_2$ . The relationship between C and electrode size (Area) satisfies equation (4) and the relationship between  $R_2$  and C satisfies equation (5). Based on the fitted values, the peak frequency calculated by the formula  $f_{peak} = 1/(2\pi\sqrt{LC})$  is similar to the original measured peak frequency, and the theoretical impedance value calculated by  $z_m \approx L/(R_2 C)$  is similar to the measured value. In summary, the circuit model has a good fit to the measured impedance values of the human upper limb region, and provides a new upper limb impedance model for obtaining various physiological information of the human body in medical research in low and medium frequency envelope electrical stimulation.

$$C = 5.577Area - 18.15 \quad (4)$$

$$R_2 = \frac{10000}{\sqrt{C}} \quad (5)$$

### Pain Perception Threshold Measurement

The relationship between pain perception and current intensity and carrier frequency was found out by adjusting the current intensity and carrier frequency, and the experiments were carried out with five sizes of electrodes. The pain perception refers to the patient's feeling, changes the above two variables, asks and observes the patient's reaction. When there is electrical stimulation, it is slightly adjusted until the sensation disappears, but there is still current output, which is recorded as subsensory threshold; when there is electrical stimulation, it is recorded as sensory threshold; when there is obvious electrical stimulation and numbness, it is recorded as supra-sensory threshold [38]. According to these three sensory criteria, the carrier frequency is adjusted within the 6~10kHz where the impedance value changes slowly, the current is adjusted within the range of 0~20mA intensity, and the step current is about 1mA.

In the process of measurement, with the increase of carrier frequency, the voltage amplitude decreases and the electrical stimulation of the subjects decreases. At this time, increasing the current will increase the voltage amplitude and enhance the electrical stimulation of the subjects. Table 5 shows the test results of one subject. For the same kind of electrode, the stan-

standard deviation of the voltage measured by the three sensations is less than 1V at different frequencies. The results showed that the electrical stimulation threshold of the subjects showed voltage consistency. In summary, the voltage at both ends of the stimulation site can replace CPT as a measure of pain perception, namely Voltage Perception Threshold (VPT).

Figure 9 shows the VPT values obtained from each electrode by sex. Figure 8a shows the perceptual threshold. Corresponding to the five electrodes, the measured values of male perception threshold are 11.04, 9.20, 6.97, 7.17 and 6.92 V, the results of female were 12.75, 9.25, 6.68, 7.13 and 6.15 V. There were significant differences between sexes when using 3.53cm<sup>2</sup> ( $P < 0.001$ ) and 50cm<sup>2</sup> ( $P < 0.01$ ) electrodes, and VPT values were consistent in the other three electrodes. Figure 8b shows the measurement results above the sensory threshold. The measured values above the threshold of male perception were 16.54, 11.36, 8.49, 8.89 and 8.51 V. The results for women were 18.58, 12.74, 8.61, 9.12 and 8.17 V. When 3.53 cm<sup>2</sup> ( $P < 0.001$ ) and 9.82 cm<sup>2</sup> ( $P < 0.001$ ) electrodes were used, there were significant differences between males and females, and the VPT values were consistent in the other three electrodes. For the measurement of sensory threshold and supra-sensory threshold, there was no significant difference in VPT value between 16cm<sup>2</sup> and 25cm<sup>2</sup> electrodes. That is to say, electrical stimulation to feel pain is determined by the voltage applied at both ends. In electrical stimulation, the conventional design is to use a constant current source circuit to achieve the therapeutic effect by controlling parameters such as current intensity and frequency. However, different individuals have different thresholds for current perception, and adopting a unified current intensity standard may have different therapeutic effects for different individuals. As a new quantitative standard, VPT value can reflect the pain of electrical stimulation more simply and accurately, and can achieve the same therapeutic effect for different individuals.

## Discussion and Conclusion

The purpose of this study is to explore the maximum value of human impedance in low-frequency envelope electrical stimulation and then determine the voltage value of power amplifier circuit of electrical stimulation equipment. The measured value of human impedance is related to the size of the electrode used and the carrier frequency of the output. When the electrode EL1 is used for electrical stimulation, the impedance range is about 0.4 to 21.6K $\Omega$ . According to figure 2a, the peak current of the output 1mA requires a power supply of 216V, while the output of 2mA requires 432V, and so on. It is unrealistic to achieve such a large voltage. The results of electrical stimulation measurement show that the voltage perceived by the human body is much less than the above-mentioned power supply value. As shown in figure 7, when the VPT exceeds about 10V, the human body has an obvious sense of electrical stimulation. The influence between different sizes of electrodes is very small, the range of sensory threshold measured from 16cm<sup>2</sup>, 25cm<sup>2</sup> and 50cm<sup>2</sup> electrodes is 6~8V, and the range of suprathreshold is 9~11V.

In addition to differentiating the test subjects by gender, we analyzed the factors affecting the impedance values of the human body using four parameters: different parts of the upper limbs of the human body, modulating wave frequency, carrier frequency, and electrode size. Only the electrode size and the output carrier frequency affect the measured value. Among them, the impedance ranges measured by different sizes of

electrodes are quite different. The human impedance circuit model shown in figure 6 fits the relationship between carrier frequency and human impedance very well. Skin impedance model was first developed by Cole [35]. Up to now, different impedance models have been proposed. Table 6 summarizes five common impedance models of the human body. The difference of the results may come from two aspects: 1. Previously, most of these models use a single waveform measurement, but this paper aims to explore the effect of human impedance on electrical stimulation parameters, and does not compare the modulated wave with a single waveform. 2. In this paper, five sizes of electrodes are utilized for the measurement of human upper limb impedance, whereas most of the previous treatises used a single electrode with unspecified dimensions and no uniform electrode material. 3. In the previous research, when the frequency range selected in the experiment is around the peak frequency, the relationship between impedance and frequency will be monotonous. If it is single increase in low frequency band, it is single decrease in high frequency band.

For the measurement of electrical stimulation perception, previous studies have suggested that the factors affecting CPT include current intensity, frequency and electrode size. It is difficult to quantify so many variables. Compared with CPT, the VPT proposed in this paper can quantify pain perception better. As shown in Figure 9, the sensory threshold and suprathreshold values obtained from electrodes EL 3, EL 4, and EL 5 are comparable. The large difference between the EL 1 and EL 2 measurements is due to their sensitivity to the measured values. As shown in Figure 6, the impedance values within 6 ~ 10 kHz have a difference of about 1.5 K $\Omega$  and 500  $\Omega$ , respectively, although the change is slower, and the sensitivity is reflected in the fact that small currents and frequency changes cause large voltage changes. The relationship between human impedance and electrical stimulation perception is not explored in this paper, but it can be seen from the above results that the measured values of these two physiological information are positively correlated.

One of the major limitations of this study is that the output intensity of electrical stimulation has not been completely measured. Clinically, the output dose of electrical stimulation therapy is determined according to the patient's sensory or muscle response [31]. Considering that subjects may have to endure uncomfortable pain during the experiment, we did not use muscle response as a basis for measuring VPT. In addition, the measurement of the impedance of the human body does not play a decisive role in the power value of the electrical stimulation power amplifier circuit. Because the final results show that the output current is not the main factor affecting the perception of electrical stimulation, the perception of electrical stimulation is only related to the voltage at both ends of the stimulation. That is no matter how much current is output, when the VPT is greater than 10V, the human body will have obvious electrical stimulation, which is far less than the product of the current and the impedance of the body. Therefore, it provides an idea of using constant voltage source circuit instead of constant current source circuit to achieve the stimulation effect for future electrical stimulation device instruments. In addition to this, we considered whether the characteristic of human upper limb impedance presenting inductance is related to the material of hydrogel electric level, and at the beginning of the experiment, we verified it with sponge electrodes as well, presenting the same tendency, which excludes the influence of hydrogel material on the impedance value.

In summary, the purpose of this paper is to measure the human impedance range and electrical stimulation sensation to determine the power supply and output intensity of electrical stimulation devices. The results show that these two parameters need to be set by considering only the electrical stimulation sensation. During the experiment, a new impedance model proposed in this study can fit the measured values well.

For electrical stimulus perception, this study proposes a new method for measuring electrical stimulus perception, i.e., Voltage Perception Threshold (VPT), based on the pattern exhibited by the measured values. VPT excludes factors such as current intensity and frequency, and only takes into account the voltages on both sides of the stimulus, which greatly simplifies the measurement criteria. Therefore, compared to CPT, VPT can provide a precise therapeutic method of electrical stimulation. In the next step of the researcher, the device developed in this study will add the voltage detection function to detect the voltage on both sides of the patient's stimulus in real time. Secondly, the method of measuring the upper limb impedance in this experiment is to utilize Ohm's law and collect the voltage at both ends of the electrode, but in fact, the upper limb impedance includes a part of electrode contact impedance, therefore, the subsequent method of measurement will be improved to exclude the effect of electrode contact impedance.

### Author Statements

### Acknowledgments

The authors would like to thank the Science and Technology Commission of Shanghai Municipality (grant number:21S31906000), the National Natural Science Foundation of China (NSFC) Grant 61803265 and Medical-industrial cross-project of USST Grant 1022308524 for founding the study.

### Research Funding

This work was supported in part by Science and Technology Commission of Shanghai Municipality (grant number:21S31906000), the National Natural Science Foundation of China (NSFC) Grant 61803265 in part by Medical-industrial cross-project of USST Grant 1022308524.

### Author Contributions

All authors have accepted responsibility for the entire content of this manuscript and approved its submission.

### Competing Interests

Authors state no conflict of interest.

### References

- Gill ML, Grahn PJ, Calvert JS, Linde MB, Lavrov IA, Strommen JA, et al. Neuromodulation of lumbosacral spinal networks enables independent stepping after complete paraplegia. *Nature Medicine*. 2018; 24: 1677-1682.
- Angeli CA, Maxwell B, Morton RA, Vogt J, Benton K, Chen Y, et al. Recovery of Over-Ground Walking after Chronic Motor Complete Spinal Cord Injury. *The New England journal of medicine*. 2018; 379: 1244-1250.
- Munoz DS, Suriano JG, Esteban EB, Farinas MV, Taylor J, Coy JA. Intensity matters: Therapist-dependent dose of spinal transcutaneous electrical nerve stimulation. *Plos one*. 2017; 12: e0189734.
- Yu-Xuan Z, Hai-Peng W, Xue-Liang B, Xiao-Ying L, Zhi-Gong W. A frequency and pulse-width co-modulation strategy for transcutaneous neuromuscular electrical stimulation based on sEMG time-domain features [J]. *Journal of neural engineering*. 2016; 13: 016004.
- Sanchez B, Pacheck A, Rutkove SB. Guidelines to electrode positioning for human and animal electrical impedance myography research. *Scientific Reports*. 2016; 6: 32615.
- Son C, Kim S, Kim S-J, Choi J, Kim D. Detection of muscle activation through multi-electrode sensing using electrical stimulation. *Sensors and Actuators: A Physical*. 2018; 275: 19-28.
- Bo S, Ramadhan BM, Nursetia DP, Tomoyuki S, Kosei N, Masahiro T. Evaluation of the effectiveness of electrical muscle stimulation on human calf muscles via frequency difference electrical impedance tomography. *Physiological Measurement*. 2021: 42.
- Shuang Q, Jing F, Rui X, Jiapeng X, Kun W, Feng H, et al. A Stimulus Artifact Removal Technique for SEMG Signal Processing During Functional Electrical Stimulation. *IEEE transactions on biomedical engineering*. 2015; 62: 1959-68.
- Qimin Y, Xiaou L, Qiaohong L. Design of functional array electrode stimulation system with surface electromyography feedback. *Journal of biomedical engineering*. 2020; 37: 1045-55.
- Ding J, Chen Z, Li Y. Development of functional electrical stimulator with real-time adjustable stimulation parameters. *Journal of Fuzhou University (Natural Science Edition)*. 2019; 47: 759-64.
- Zhou Y, Fang Y, Gui K, Li K, Zhang D. Honghai Liu. sEMG Bias-driven Functional Electrical Stimulation System for Upper-Limb Stroke Rehabilitation. *IEEE Sensors Journal*. 2018; 1-1.
- Sanchez B, Aroul P, Lourdes A, Bartolome E, Soundarapandian K, Bragos R. Propagation of Measurement Errors Through Body Composition Equations for Body Impedance Analysis. *IEEE Transactions on Instrumentation and Measurement*. 2014; 63: 1535-44.
- Koyu C, Ichiko K, Aki Z, Kotoyo I, Kanako N. New equivalent-electrical circuit model and a practical measurement method for human body impedance. *Bio-medical materials and engineering*. 2015; 26: S779-86.
- Freeborn TJ, Elwakil AS, Maundy B, Trujillo JJ. Compact Wide Frequency Range Fractional-Order Models of Human Body Impedance against Contact Currents. *Mathematical Problems in Engineering*. 2016; 2016.
- Demir U, Kocaoğlu S, Akdoğan E. Human impedance parameter estimation using artificial neural network for modelling physiotherapist motion. *Biocybernetics and Biomedical Engineering*. 2016; 36: 318-326.
- Shiffman C. Scaling and the frequency dependence of Nyquist plot maxima of the electrical impedance of the human thigh. *Physiological Measurement*. 2017; 38: 2203-2221.
- Kubisz L, Hojan-Jeziarska D, Szewczyk M, Majewska A, Kawałkiewicz W, Pankowski E, et al. In vivo electrical impedance measurement in human skin assessment[J]. *Pure and Applied Chemistry*. 2019; 91.
- Jyoti BD, Rajdeep D. Estimation of skin impedance models with experimental data and a proposed model for human skin impedance. *IET Systems Biology*. 2020; 14: 230-240.
- Srdjan R, Vojislav VM, Goran L. Neural Networks Application on Human Skin Biophysical Impedance Characterizations. *Biophysical Reviews and Letters*. 2021; 16: 9-19.

20. Rutkove SB. Electrical impedance myography: Background, current state, and future directions[J]. *Muscle & nerve*. 2009; 40: 936-946.
21. Lely S, Liechti MD, Bachmann LM, Kessler TM, Mehnert U. Quantitative electrical pain threshold assessment in the lower urinary tract[J]. *Neurourology and Urodynamics*. 2020; 39: 420-431.
22. Seno SI, Shimazu H, Kogure E, Watanabe A, Kobayashi H. Factors Affecting and Adjustments for Sex Differences in Current Perception Threshold with Transcutaneous Electrical Stimulation in Healthy Subjects. *Neuromodulation: Technology at the Neural Interface*. 2019; 22: 573-579.
23. Joon OK, Hoon KS, Young-Hee L, Heon KJ, Sun JH, Jun PT, et al. Pain-related evoked potential in healthy adults. *Annals of rehabilitation medicine*. 2015; 39: 108-115.
24. Ji-Ri-Mu-Tu-Ya, Yin Y, Zhu T. Determination of Electrical Stimulation Pain Perception and Analysis of the Related Factors. *Journal of Biomedical Engineering*. 2013; 30: 1200-8.
25. Chang W, Xu W, Hu R, An Y. Current Perception Threshold Testing in Pharyngeal Paresthesia Patients with Depression or Anxiety. *Neuropsychiatric Disease and Treatment*. 2020; 16: 1023-1029.
26. Suzuki Y, Muramatsu K, Maruo K, Kato H, Tanabe Y, Tubaki T, et al.. Pain thresholds are unaffected by age in a Japanese population. *Muscle & Nerve*. 2020: 61.
27. Solomons CD, Slovak M, Heller B, Barker AT. Reducing the sensation of electrical stimulation with dry electrodes by using an array of constant current sources. *Medical Engineering and Physics*. 2018; 51: 91-95.
28. Chan SCC, Peng J, Chan CCH. Reliability of measurements for sub-painful and painful perception on artificial electrical stimulations. *International Journal of Psychophysiology*. 2018; 123: 35-41.
29. Furuse N, Kimoto S, Nakashima Y, Ogawa T, Furokawa S, Okubo M, et al. Verification of the reliability of current perception threshold and pain threshold testing by application of an electrical current stimulus to mandibular mucosa in young adults. *Journal of Oral Rehabilitation*. 2019; 46: 556-562.
30. Seno SI, Shimazu H, Kogure E, Watanabe A, Kobayashi H. Factors Affecting and Adjustments for Sex Differences in Current Perception Threshold with Transcutaneous Electrical Stimulation in Healthy Subjects. *Neuromodulation: Technology at the Neural Interface*. 2019; 22: 573-579.
31. Ying S, Zhiqiang Z. *Clinical work guidelines for rehabilitation therapists - physical factor therapy techniques*. Beijing: People's Health Publishing House. 2019.
32. Son C, Kim S, Kim SJ, Choi J, Kim D. Detection of muscle activation through multi-electrode sensing using electrical stimulation. *Sensors and Actuators: A Physical*. 2018; 275.
33. Cole KS, Curtis HJ. Electric impedance of nerve and muscle. *Cold Spring Harb Symp Quant Biol*. 1936; 4: 73-89.
34. Mihaela G, Martine N, Jasper J, Dana C, Muresan CI, Ionescu CM. Bioimpedance Sensor and Methodology for Acute Pain Monitoring. *Sensors*. 2020; 20: 6765.